Integrating mitochondrial energetics, redox and ROS metabolic networks: A two-compartment model*

Jackelyn M. Kembro[*], Miguel A. Aon[*], Raimond L. Winslow[†], Brian O'Rourke[*] and Sonia Cortassa[*, †]

[*]Division of Cardiology, and [†]Institute for Computational Medicine

Johns Hopkins University School of Medicine, Baltimore MD 21205

Supporting Material

Section S1. Redox potential and Redox environment

The Nernst equation was used to estimate the redox potential of each redox couple. The Nernst equation relates the change in free energy of the transfer of electrons to the voltage of an electrochemical cell, and can be expressed as:

$$\Delta E = \Delta E° - \frac{RT}{nF} \ln Q \qquad \text{(S1)}$$

where n is the number of electrons exchanged in the chemical process, F is the Faraday constant, and ΔE° is the electromotive force under standard conditions, that is, the difference in the standard reduction potentials of the two half-cells involved in the process. The superscript ° implies the thermodynamic standard state. Q stands for the ratio of the concentration of products over the concentration of substrates of the redox reaction. When ΔE is zero, thus ΔG is zero, there is no net electron flow. Since, pH in the mitochondrial is not 7, Eq. 2 must be corrected for pH (Eq. 3) (for further explanation refer to (1)). The Nernst equation for 37°C (310°K), using 2.303 as the conversion factor for *ln* into *log10* is:

$$E = E° + \left(\left(pH - 7 \right) * \left(-61.51\text{mV} \right) \right) - \frac{61.51\text{mV}}{n} \log \frac{\left[\text{Red}_1 \right]}{\left[\text{Ox}_1 \right]} \qquad \text{(S2)}$$

The standard redox potentials used were -320 mV NADH/NAD^+, -324 mV for NADPH/$NADP^+$ (E° = -324) mV, -292 mV for $Trx(SH)_2$/TrxSS, and -240 mV for (2 GSH)/GSSG.

The ***redox environment*** was calculated from the summation of the products of the reduction potential and reducing capacity of the linked redox couples present in the system (1):

$$Redox\,environment = \sum_{i=1}^{n(couple)} E_i \; [reduced\ species]_i \qquad \text{(S3)}$$

being E_i is the half-cell reduction potential (Nernst potential, Eq. 3) for a given redox pair and $[\text{reduced species}]_i$ is the concentration of the reduced species in that redox pair (conceptually developed under Results section "*Steady state behavior of the redox environment").*

Section S2

B

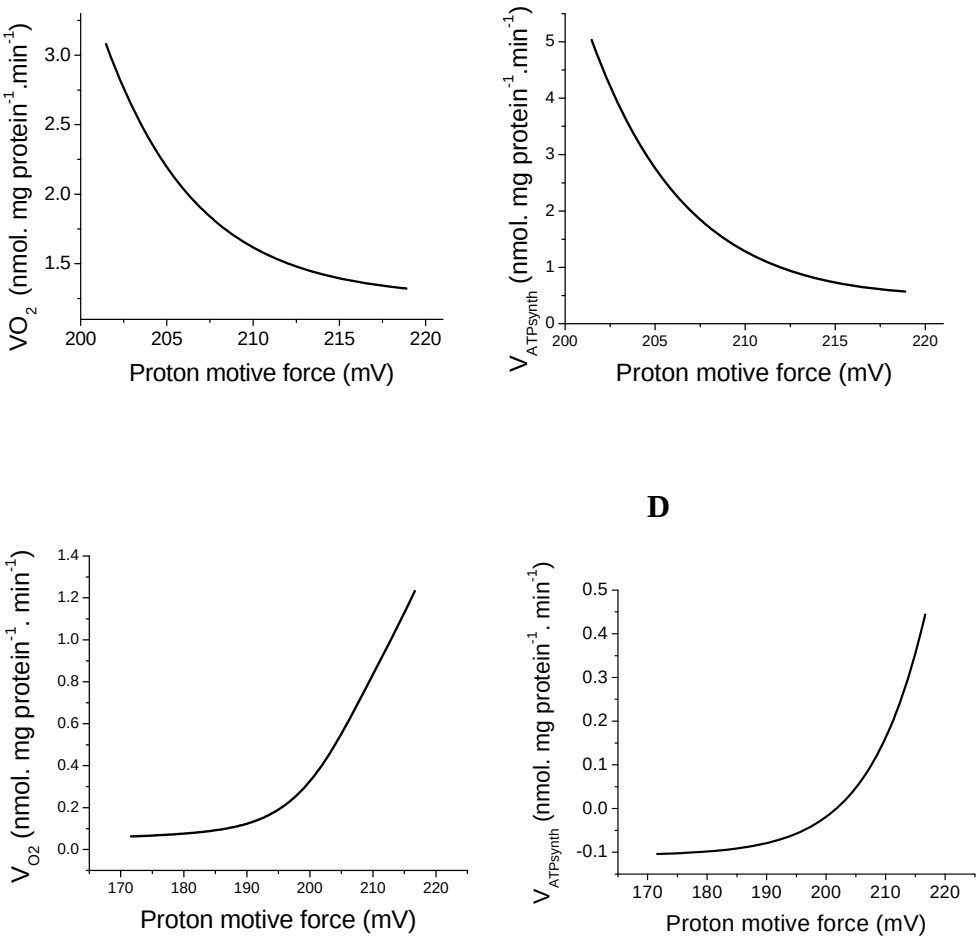

Fig. S1. Steady state respiratory flux and ATP synthase activity

Steady state A) respiration from both complex I and II (VO_2) and C) ATP synthase rate *versus* proton motive force, obtained by departing from a state 4 respiratory state ($[ADP]_i = 0.01$ mM) and increasing the extra-mitochondrial ADP concentration towards a state 3 respiratory state ($[ADP]_i$=1 mM). (C) and (D) Steady state flux of respiration and ATP synthase rate, respectively, as related with proton motive force, obtained by departing from a de-energized steady state and increasing the parameter [AcCoA] from 1×10^{-6} to 1 mM, at a fixed GLU concentration of 1.3×10^{-4} mM, and $[ADP]_i = 0.01$ mM.

Section S3. Oscillatory dynamics in the ME-R model

Stability analysis of the model was performed as a function of the fraction of electrons channeled from the respiratory chain into $O_2^{\cdot-}$ production versus respiration at different levels of matrix superoxide dismutase (MnSOD) activity. The model simulates the experimentally determined oscillatory period, $\Delta\Psi_m$/NADH phase relationship, and the typical waveform exhibited by relaxation oscillators (Fig. S2) (2, 3).

The underlying oscillatory mechanism involves ROS imbalance determined by the interplay between ROS production and scavenging (SOD) as the main trigger. During an oscillatory cycle,

accumulation of $O_2^{\cdot -}$ in the mitochondrial matrix augments the leak through the inner membrane anion channel (IMAC). When the level of extra-matrix $O_2^{\cdot -}$ (dashed line in Fig. S2) exceeds a threshold it triggers the opening of IMAC. As a result, $\Delta\Psi_m$ depolarizes concomitant with oxidation of the NADH pool (Fig. S2). The cycle terminates when $O_2^{\cdot -}$ drops below the threshold, subsequent to scavenger pathway activation and decreased $O_2^{\cdot -}$ efflux. The ability of the ME-R model to simulate the mitochondrial oscillations is remarkable, given that the levels of $O_2^{\cdot -}$ attained during an oscillatory cycle are much lower than in previous simulations (3) . The bi-compartmental nature of the new model which accounts for both ROS scavenging in the matrix and extra-matrix space (see Fig. 1), also testifies to the robustness of the oscillatory mechanism.

A

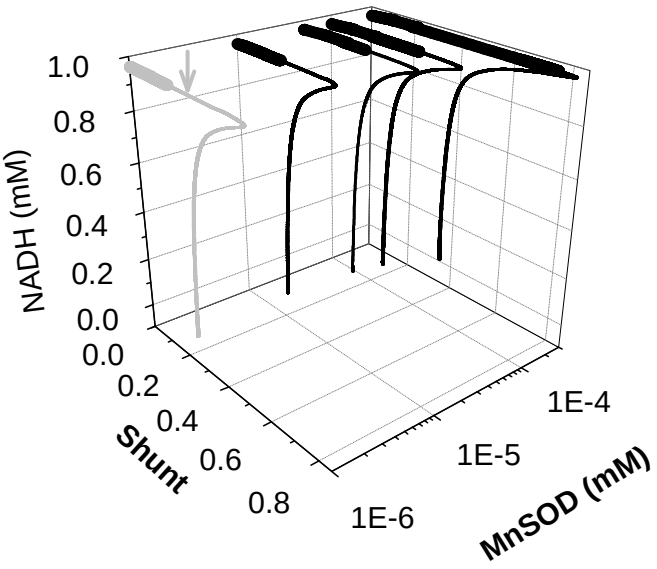

B

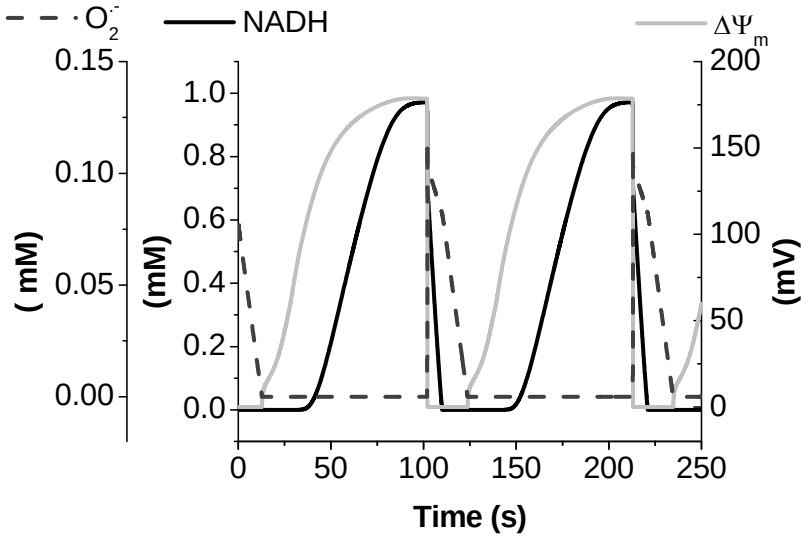

Fig. S2. Simulation of sustained mitochondrial oscillations under oxidative stress

A) 3D representation of bifurcation diagrams of NADH as a function of the rate of ROS production by the respiratory chain (shunt) and ROS scavenging given by various levels of Mn SOD (Et_{MnSOD}). Thick lines indicate domains of stable steady-state behavior, whereas thin lines denote either unstable or oscillatory states. The stable oscillatory domain in the upper branch widens as MnSOD concentration decreases. Unstable regions are characterized by, at least, one pair of complex conjugate eigenvalues with positive real parts. From left to right, the MnSOD concentration was (in mM): 1×10^{-6}, 1×10^{-5}, 5×10^{-5}, 1×10^{-4} and 3×10^{-4}. A Cu,ZnSOD concentration of 3.2×10^{-4} mM was used in all (4) but one of the curves where a concentration of 4×10^{-4} was utilized (grey trace). Notice that the appearance of sustained mitochondrial oscillations is nonlinearally dependent on both the rate of ROS production by the respiratory chain and scavenging of $O_2^{\cdot-}$ by MnSOD and Cu, ZnSOD.

B) Simulation of sustained mitochondrial oscillations with a period of ~ 100s. Parameters used were Shunt= 0.25; $Et_{MnSOD}=1\times10^{-6}$; $Et_{CuZnSOD}=4\times10^{-4}$ (indicated with a grey arrow in panel A). Simulations were performed with following parameter set: $\rho^{F1}=0.02$, $\rho^{res}=0.018$, $\rho^{res(SDH)}=0.007$, $[Pi]_I=0.5$, [AcCoA]= 0.01, [GLU]= 10, $g_H=3\times10^{-8}$, $k_{cat}^{CS}=7.84\times10^{-6}$, $k_f^{ACO}=3.896\times10^{-6}$, $k_{cat}^{IDH}=2.64\times10^{-2}$, $k_{cat}^{KDGH}=8.84\times10^{-4}$, $k_f^{SL}=1.40\times10^{-3}$, $k_f^{FH}=4.15\times10^{-4}$, $k_{cat}^{MDH}=6.21\times10^{-3}$, $k_f^{AAT}=1.07\times10^{-3}$, $c_{PiC}=1.69$, Vnai =5, $V_{max}^{uni}=2.46\times10^{-3}$, $V_{max}^{NaCa}=9.33\times10^{-5}$, $V_{maxANT}=0.4354$, $E_T^{TrxR2m}=8.7\times10^{-5}$, $E_T^{TrxR1}=8.7\times10^{-5}$, $E_T^{Prx3m}=8\times10^{-3}$, $E_T^{Prx1}=5\times10^{-3}$, $E_T^{GPXm}=5\times10^{-6}$, $E_T^{GPX1}=0.001$, $E_T^{GRm}=1.6\times10^{-4}$, $E_T^{GR1}=1.6\times10^{-4}$, $E_{CAT}^T=1\times10^{-6}$.

Section S4.

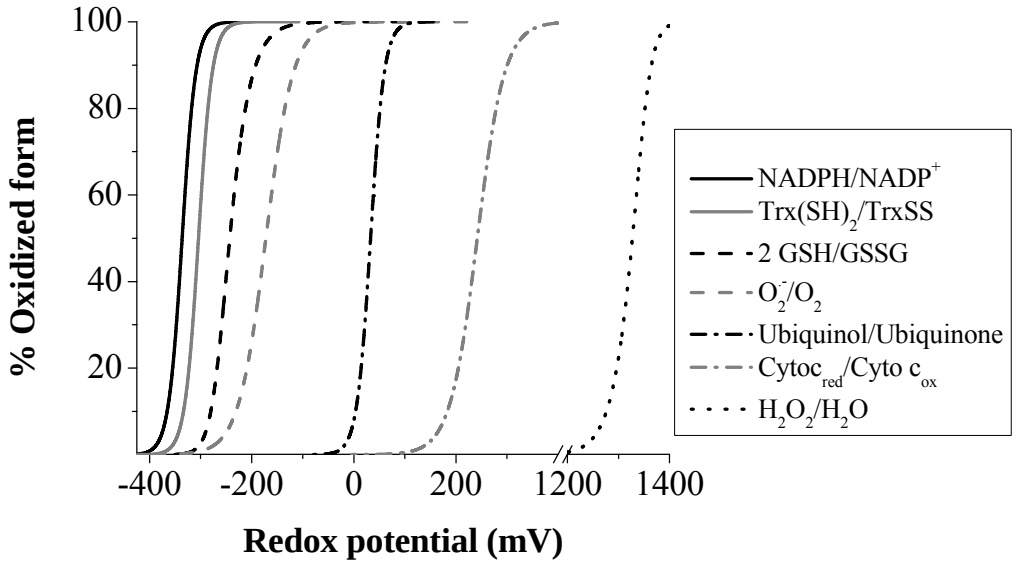

Fig. S3. Reduction potential of main mitochondrial redox couples

From this representation it can be clearly seen that the $NADP^+$/NADPH couple is the provider of reducing equivalents needed by GSH/Trx scavenging systems to reduce H_2O_2 to water, in a thermodynamically highly favorable reaction. Percent oxidized form = ([oxidized]/total)*100. Considering the basic redox reaction: $\mathbf{Red_1} + Ox_2 \leftrightarrow \mathbf{Ox_1} + Red_2$, for each redox couple Red_1 varied from 1×10^{-4} to 1 mM while Ox_1 was estimated as 1 - Red_1. The standard redox potentials used in this graph were -324 mV for NADPH/$NADP^+$; -292 mV for $Trx(SH)_2$/TrxSS; -240 mV for 2 GSH/GSSG; -160 mV for $O_2^{\cdot-}/O_2$; 45 mV for Ubiquinol/Ubiquinone; 254 mV for Cytochrome c (Fe^{3+})/ Cytochrome c (Fe^{2+}) and 1349 mV for H_2O_2 (1, 5, 6). Concentrations were varied between $1x10^{-4}$ and 1. Conditions correspond to pH 7.2 and 37°C.

Section S5. Relationship between NADH concentration and membrane potential ($\Delta\Psi_m$) at different level of substrates

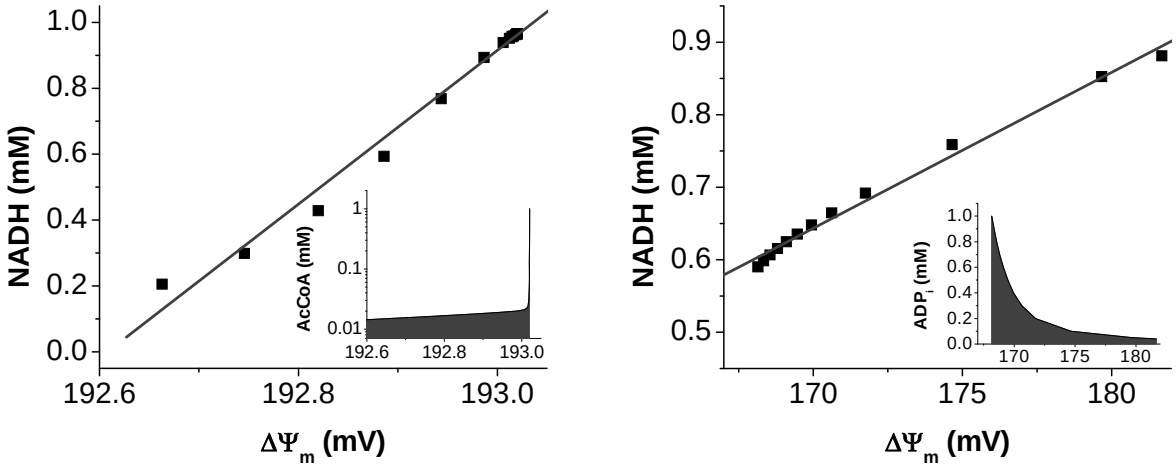

Fig. S4. Lineal relationship between NADH and $\Delta\Psi_m$ at different concentrations of Acetyl CoA (AcCoA) and ADP

A) Steady state values of NADH and $\Delta\Psi_m$ were obtained at increasing concentrations of AcCoA (inset). B) Steady state values of NADH and $\Delta\Psi_m$ were obtained at increasing concentrations of ADP_i (inset). From this representation it can be clearly seen that increasing concentrations of extra-matrix ADP (simulating state 4 to sate 3 transition) results in decrease of both NADH and $\Delta\Psi_m$, while a lineal relationship is maintained between these variables. The parameter set used is the same as in the simulations presented in the main text.

Section S6

Table S1. System of differential and algebraic equations used in the ME-R model

$\frac{d[Ca^{2+}]_m}{dt} = \delta_{Ca}\left(V_{uni} - V_{NaCa}\right)$	(S4)
$\frac{d\,[ADP]_m}{dt} = V_{ANT} - V_{ATPase} - V_{SL}$	(S5)
$\frac{d\Delta\Psi_m}{dt} = \frac{V_{He} + V_{He(SDH)} - V_{Hu} - V_{ANT} - V_{Hleak} - V_{NaCa} - V_{uni} - V_{IMAC}}{C_{mito}}$	(S6)
$\frac{d[NADH]_m}{dt} = V_{O_2} + V_{IDH} + V_{KGDH} + V_{MDH} - V_{THD}$	(S7)
$\frac{d[H^+]_m}{dt} = \delta_M\left(-V_{He} - V_{He(SDH)} + V_{Hu} + V_{NaH} + V_{PiC} + V_{Hleak}\right)$	(S8)
$\frac{d[Pi]_m}{dt} = -V_{ATPase} + V_{PiC} - V_{SL}$	(S9)
$\frac{d[ISOC]}{dt} = V_{ACO} - V_{IDH} - V_{IDH\_NADP}$	(S10)
$\frac{d[\alpha KG]}{dt} = V_{IDH} + V_{IDH\_NADP} - V_{KGDH} + V_{ATT}$	(S11)
$\frac{d[SCoA]}{dt} = V_{KGDH} - V_{SL}$	(S12)
$\frac{d[Suc]}{dt} = V_{SL} - V_{O_2SDH}$	(S13)
$\frac{d[FUM]}{dt} = V_{O_2SDH} - V_{FH}$	(S14)
$\frac{d[MAL]}{dt} = V_{FH} - V_{MDH}$	(S15)
$\frac{d[OAA]}{dt} = V_{MDH} - V_{CS} - V_{AAT}$	(S16)
$\frac{d[NADPH]_m}{dt} = V_{IDH\_NADP} + V_{THD} - V_{GRm} - V_{TxRm}$	(S17)

$$\frac{d[O_2^{\bullet-}]_m}{dt} = shunt\left(V_{O_2} + V_{O_2SDH}\right) - V_{MnSOD} - V_{ROS}^{Tr} \quad \text{(S18)}$$

$$\frac{d[O_2^{\bullet-}]_i}{dt} = \frac{v_m}{v_i} V_{ROS}^{Tr} - V_{CuZnSOD} \quad \text{(S19)}$$

$$\frac{d[H_2O_2]_m}{dt} = V_{MnSOD} - V_{difH_2O_2} - V_{GPXm} - V_{TxPXm} \quad \text{(S20)}$$

$$\frac{d[H_2O_2]_i}{dt} = V_{CuZnSOD} + \frac{v_m}{v_i} V_{difH_2O_2} - V_{GPXi} - V_{TxPXi} - V_{CAT} \quad \text{(S21)}$$

$$\frac{d[GSH]_m}{dt} = V_{GRm} - V_{GPXm} - V_{GRXm} + V_{GST} - V_{PSSGm} \quad \text{(S22)}$$

$$\frac{d[GSH]_i}{dt} = V_{GRi} - V_{GPXi} - V_{GRXi} + \frac{v_m}{v_i} V_{GST} - V_{PSSGi} \quad \text{(S23)}$$

$$\frac{d[GSSG]_m}{dt} = 0.5\left(V_{GPXm} - V_{GRm}\right) + V_{GRXm} \quad \text{(S24)}$$

$$\frac{d[TxR]_m}{dt} = V_{TxRm} - V_{TxPXm} \quad \text{(S25)}$$

$$\frac{d[TxR]_i}{dt} = V_{TxRi} - V_{TxPXi} \quad \text{(S26)}$$

$$\frac{d[PSSG]_m}{dt} = V_{PSSGm} - V_{GRXm} \quad \text{(S27)}$$

$$\frac{d[PSSG]_i}{dt} = V_{PSSGi} - V_{GRXi} \quad \text{(S28)}$$

The values of the ratio v_m/v_i used, representing the volume of the mitochondrial matrix (v_m) over the extra-matrix compartment (v_i), were 0.00256 to represent the cuvette situation or 0.25 for the intracellular condition.

Section S7. Computational modeling of Reactive Oxygen Species scavenging systems

The upgraded two-compartment computational model of mitochondrial energetics-redox (ME-R) includes: (i) a complete array of antioxidant defenses in two compartments: mitochondrial matrix and extra-matrix (e.g. intermembrane space, cytoplasm); and (ii) two of the three main NADPH providers in mitochondria: $NADP^+$-dependent isocitrate dehydrogenase (IDH2) in the TCA cycle, and transhydrogenase (THD). In this section we will provide a detailed description of the antioxidant defenses and mitochondrial NADPH handling.

7.1. Modeling superoxide dismutase

$$V_{MnSOD} = \frac{2\, k^1_{SOD}\, k^5_{SOD}\left(k^1_{SOD} + k^3_{SOD}\left(1 + \frac{[H_2O_2]_m}{K_i^{H_2O_2}}\right)\right) E^T_{MnSOD}\,[O_2^{\bullet -}]_m}{k^5_{SOD}\left(2\, k^1_{SOD} + k^3_{SOD}\left(1 + \frac{[H_2O_2]_m}{K_i^{H_2O_2}}\right)\right) + [O_2^{\bullet -}]_m\, k^1_{SOD}\, k^3_{SOD}\left(1 + \frac{[H_2O_2]_m}{K_i^{H_2O_2}}\right)} \quad \text{(S29)}$$

$$V_{CuZnSOD} = \frac{2\, k^1_{SOD}\, k^5_{SOD}\left(k^1_{SOD} + k^3_{SOD}\left(1 + \frac{[H_2O_2]_i}{K_i^{H_2O_2}}\right)\right) E^T_{CuZnSOD}\,[O_2^{\bullet -}]_i}{k^5_{SOD}\left(2\, k^1_{SOD} + k^3_{SOD}\left(1 + \frac{[H_2O_2]_i}{K_i^{H_2O_2}}\right)\right) + [O_2^{\bullet -}]_i\, k^1_{SOD}\, k^3_{SOD}\left(1 + \frac{[H_2O_2]_i}{K_i^{H_2O_2}}\right)} \quad \text{(S30)}$$

7.2. H_2O_2 transport

H_2O_2 can diffuse freely between the two compartments, following the equation:

$$V_{diff_{H_2O_2}} = C_{diff_{H_2O_2}}\left([H_2O_2]_m - [H_2O_2]_i\right) \quad \text{(S31)}$$

7.3. Gluthathione and glutaredoxin systems

The gluthathione system was present in both mitochondrial matrix and extra-matrix compartments and expressed as a system of equations comprising glutathione peroxidase (V_{GPx}) and reductase (V_{GR}) activities. The rate expressions for V_{GPx} and V_{GR} used in the model were formulated as described in our mitochondrial model of ROS metabolism (3).

$$V_{GPX_m} = \frac{E_T^{GPXm}[H_2O_2]_m[GSH]_m}{\Phi_1[GSH]_m + \Phi_2[H_2O_2]_m} \quad \text{(S32)}$$

$$V_{GPX_i} = \frac{E_T^{GPXi}[H_2O_2]_i[GSH]_i}{\Phi_1[GSH]_i + \Phi_2[H_2O_2]_i} \quad \text{(S33)}$$

$$V_{GR_m} = \frac{k_{\mathrm{GR}}^{1}\ \mathrm{E}_{T}^{\mathrm{GRm}}}{1+\frac{K_M^{\mathrm{GSSG}}}{[\mathrm{GSSG}]}+\frac{K_M^{\mathrm{NADPH}}}{[\mathrm{NADPH}]_{\mathrm{m}}}+\frac{K_M^{\mathrm{GSSG}}}{[GSSG]_m}\frac{K_M^{\mathrm{NADPH}}}{[\mathrm{NADPH}]_{\mathrm{m}}}} \quad \text{(S34)}$$

$$V_{GR_i} = \frac{k_{\mathrm{GR}}^{1}\ \mathrm{E}_{T}^{\mathrm{GRi}}}{1+\frac{K_M^{\mathrm{GSSG}}}{\mathrm{V}_{GSS}}+\frac{K_M^{\mathrm{NADPH}}}{[\mathrm{NADPH}]_{\mathrm{i}}}+\frac{K_M^{\mathrm{GSSG}}}{[GSSG]_i}\frac{K_M^{\mathrm{NADPH}}}{[\mathrm{NADPH}]_{\mathrm{i}}}} \quad \text{(S35)}$$

The glutaredoxin system can then detoxify the glutathionylated proteins and uses GSH as cofactor (7, 8).

$$V_{GRX_m} = \frac{k_{grx_m}\ K_{eq}^{GRX}\left([GSH]_m\right)^2\ GrxT\ [PSSG]_m}{\left([\mathrm{GSSG}]_{\mathrm{m}}+K_{eq}^{GRX}\left([GSH]_m\right)^2\right)\left(\frac{K_{eq}^{GRX}\left([GSH]_m\right)^2\ GrxT}{[\mathrm{GSSG}]_{\mathrm{m}}+K_{eq}^{GRX}\left([GSH]_m\right)^2}+K_m^{Grx}\right)\left([\mathrm{PSSG}]_{\mathrm{m}}+K_m^{PSSG}\right)} \quad \text{(S36)}$$

$$V_{GRX_i} = \frac{k_{grx_i}\ K_{eq}^{GRX}\left([GSH]_i\right)^2\ GrxT\ [PSSG]_i}{\left(\mathrm{V}_{\mathrm{GSS}}+K_{eq}^{GRX}\left([GSH]_i\right)^2\right)\left(\frac{K_{eq}^{GRX}\left([GSH]_i\right)^2\ GrxT}{[GSSG]_i+K_{eq}^{GRX}\left([GSH]_i\right)^2}+K_m^{Grx}\right)\left([\mathrm{PSSG}]_{\mathrm{i}}+K_m^{PSSG}\right)} \quad \text{(S37)}$$

$$V_{PSSG_m} = \frac{k_{\mathrm{PSH}}^{1}\ \mathrm{E}_{T}^{\mathrm{PSH}}\ (PSSGT-[PSSG]_m)}{\left(1+\frac{K_M^{GSH}}{[GSH]_m}\right)\left(1+\frac{[H_2O_2]_m}{K_{act}^{H2O2}}\right)} \quad \text{(S38)}$$

$$V_{PSSG_i} = \frac{k_{\mathrm{PSH}}^{1}\ \mathrm{E}_{T}^{\mathrm{PSH}}\ (PSSGT-[PSSG]_i)}{\left(1+\frac{K_M^{GSH}}{[GSH]_i}\right)\left(1+\frac{[H_2O_2]_i}{K_{act}^{H2O2}}\right)} \quad \text{(S39)}$$

We have assumed that the total pool of glutathione, G_T, is conserved, as indicated by equation S40, and from there the GSSG concentration in the extra-matrix compartment can be estimated (Eq. S41).

$$\mathrm{G}_T = \mathrm{G}_T - [\mathrm{GSH}]_{\mathrm{m}} - [\mathrm{GSH}]_i - 2[\mathrm{GSSG}] - [\mathrm{PSSG}]_{\mathrm{m}} - [\mathrm{PSSG}]_{\mathrm{i}} - 2[GSSG]_i \quad \text{(S40)}$$

$$[\mathrm{GSSG}]_i = 0.5\left(\mathrm{G}_T - [\mathrm{GSH}]_{\mathrm{m}} - [\mathrm{GSH}]_i - 2[\mathrm{GSSG}]_{\mathrm{m}} - [\mathrm{PSSG}]_{\mathrm{m}} - [\mathrm{PSSG}]_{\mathrm{i}}\right) \quad \text{(S41)}$$

In addition we have included passive GSH transport (V_{GST}) across the inner mitochondrial membrane.

$$V_{GST} = c_{GST} \frac{\left([GSH]_i - [GSH]_m \right)}{[GSH]_i + k_{0.5}^{GST}} \quad \text{(S42)}$$

7.4. Thioredoxin system

The Trx system includes peroxiredoxin (V_{TxPX}) and thioredoxin reductase (V_{TxR}) (9). The rate expression for V_{TPrx3} was derived on the basis of the experimental studies performed by (10), from which we also obtained the rate constants. V_{TxR} represents a Michaelis-Menten rate expression with two substrates (NADPH and Trx(SS) with kinetic parameters derived from refs. (11) and (12).

$$V_{TxPX_m} = \frac{E_T^{Prx3m} [H_2O_2]_m \ [TrxSH_2]_m}{\Phi_{1Prx} [TrxSH_2]_m + \Phi_{2Prx} [H_2O_2]_m} \quad \text{(S43)}$$

$$V_{TxPX_i} = \frac{E_T^{Prxi} [\mathrm{H_2O_2}]_\mathrm{i} [\mathrm{TrxSH_2}]_\mathrm{i}}{\Phi_{1Prx} [\mathrm{TrxSH_2}]_\mathrm{i} + \Phi_{2Prx} [\mathrm{H_2O_2}]_i} \quad \text{(S44)}$$

$$V_{TxR_m} = \frac{k_{\mathrm{TrxR}}^1 \ \mathrm{E}_T^{Trx\mathrm{R2m}}}{1 + \frac{K_M^{\mathrm{TrxSS}}}{[TrxSS]_m} + \frac{K_{Mtrx}^{\mathrm{NADPH}}}{[NADPH]_m} + \frac{K_M^{\mathrm{TrxSS}}}{[TrxSS]_m} \frac{K_{Mtrx}^{\mathrm{NADPH}}}{[NADPH]_m}} \quad \text{(S45)}$$

$$V_{TxR_i} = \frac{k_{\mathrm{TrxR}}^1 \ \mathrm{E}_T^{\mathrm{TrxRi}}}{1 + \frac{K_M^{\mathrm{TrxSS}}}{[TrxSS]_i} + \frac{K_{Mtrx}^{\mathrm{NADPH}}}{[NADPH]_i} + \frac{K_M^{\mathrm{TrxSS}}}{[TrxSS]_i} \frac{K_{Mtrx}^{\mathrm{NADPH}}}{[NADPH]_i}} \quad \text{(S46)}$$

$$[\mathrm{TrxSS}]_\mathrm{m} = TrxT_m - [\mathrm{TrxSH_2}]_\mathrm{m} \quad \text{(S47)}$$

$$[\mathrm{TrxSS}]_\mathrm{i} = TrxT_i - [\mathrm{TrxSH_2}]_\mathrm{i} \quad \text{(S48)}$$

7.5. Extra-matrix Catalase

$$V_{CAT} = 2 k_{CAT}^1 E_{CAT}^T [\mathrm{H_2O_2}]_\mathrm{i} e^{-fr[\mathrm{H_2O_2}]_\mathrm{i}} \quad \text{(S49)}$$

Table S2. Parameter values used in the simulations: ROS production and scavenging

Symbol	Value	Units	Description	Eq	Reference
k_{SOD}^{1}	1.2×10^{3}	$mM^{-1}ms^{-1}$	Second-order rate constant of SOD	S29,S30	
k_{SOD}^{3}	24	$mM^{-1}ms^{-1}$	Second-order rate constant of SOD	S29,S30	
k_{SOD}^{5}	2.4×10^{-4}	ms^{-1}	First-order rate constant of SOD	S29,S30	
$K_{i}^{H_2O_2}$	0.5	mM	Inhibition constant for H_2O_2	S29,S30	f
E_{MnSOD}^{T}	T. 1	mM	Mitochondrial matrix concentration of MnSOD	S29	Adjusted
$E_{CuZnSOD}^{T}$	T. 1	mM	Concentration of Cu,ZnSOD	S30	Adjusted
$c_{diff_{H_2O_2}}$	2×10^{-4}	ms^{-1}	Diffusion constant for H_2O_2	S31	Adjusted
Φ_1	5.0×10^{-3}	mM ms	Constant for GPX activity	S32,S33	a
Φ_2	0.75	mM ms	Constant for GPX activity	S32,S33	a
E_T^{GPXm}	T. 1	mM	Mitochondrial matrix concentration of GPX	S32	Adjusted
E_T^{GPXi}	T. 1	mM	Extra-matrix concentration of GPX	S33	Adjusted
k_{GR}^{1}	2.5×10^{-3}	ms^{-1}	Catalytic constant of GR	S34,S35	a
E_T^{GRm}	T. 1	mM	Mitochondrial matrix concentration of GR	S34	Adjusted
E_T^{GRi}	T. 1	mM	Extra-matrix concentration of GR	S35	Adjusted
K_M^{NADPH}	0.015	mM	Michaelis constant for NADPH of GR	S34,S35	a
K_M^{GSSG}	0.06	mM	Michaelis constant for GSSG of GR	S34,S35	a
$[NADPH]_i$	7.5×10^{-2}	mM	Extra-matrix NADPH concentration	S34,S35	
G_T	6	mM	Total pool of glutathione	S40,S41	a
k_{grx_m}	3.6×10^{-4}	mM s^{-1}	Rate constant of mitochondrial matrix glutaredoxin reaction	S36	Adjusted

k_{grx_i}	3.6×10^{-4}	mM s^{-1}	Rate constant of extra-matrix glutaredoxin reaction	S37	Adjusted
K_{eq}^{GRX}	1.37×10^{-3}	mM^{-1}	Equilibrium constant of glutaredoxin	S36,S37	
K_m^{Grx}	0.01	mM	Michaelis constant for GSH of GRX	S36,S37	
K_m^{PSSG}	0.0005	mM	Michaelis constant for glutathionylated protein of glutaredoxin	S36,S37	
k_{PSH}^{1}	0.64	ms^{-1}	Rate constant of protein glutathionylation	S38,S39	
$\mathrm{E}_T^{\mathrm{PSH}}$	8×10^{-4}	mM	Concentration of proteins that can become glutathionylated	S38,S39	
K_M^{GSH}	0.75	mM	Michaelis constant of GSH for glutathionylation	S38,S39	
K_{act}^{H2O2}	1×10^{-3}	mM	Activation constant of H_2O_2 for protein glutathionylation	S38,S39	
$GrxT$	0.002	mM	Glutaredoxin concentration	S38,S39	
c_{GST}	1.5×10^{-8}	ms^{-1}	Rate constant of glutathione transporter	S42	
$k_{0.5}^{GST}$	2.6	mM	transport association constant of GSH	S42	
E_T^{Prx3m}	T. 1	mM	Mitochondrial matrix concentration of Trx peroxidase (Prx)	S43	Adjusted
E_T^{Prx3i}	T. 1	mM	Extra-matrix concentration Prx	S44	Adjusted
Φ_{1Prx}	3.83	mM ms	Constant for TxPX activity	S43,S44	b
Φ_{2Prx}	1.85	mM ms	Constant for TxPX activity	S43,S44	b
E_T^{TrxR2m}	T. 1	mM	Mitochondrial matrix concentration of TrxR2	S45	
E_T^{TrxRi}	T. 1	mM	Extra-matrix concentration of TrxR	S46	
K_M^{TrxSS}	0.035	mM	Michaelis constant for oxidized Trx [Trx(SS)] of TrxR	S45,S46	d,e
$\mathrm{K}_{Mtrx}^{NADPH}$	0.012	mM	Michaelis constant for NADPH of Trx	S45,S46	d,e

	22.7×10^{-3}	ms^{-1}	Rate constant of TrxR	S45,S46	d,e
k^1_{TrxR}					
$TrxT_m$	0.025	mM	Total pool of mitochondrial matrix thioredoxin	S47	c
	0.05	mM	Total pool of extra-matrix thioredoxin	S48	
$TrxT_i$					
k^1_{CAT}	17	$mM^{-1}ms^{-1}$	Rate constant of catalase (CAT)	S49	
E^T_{CAT}	1.0×10^{-6}	mM	Extra-matrix concentration of CAT	S49	
fr	5.0×10^{-2}	mM^{-1}	Hydrogen peroxide inhibition factor of CAT	S49	

(a) (3); *(b)* (10); *(c)* (9); *(d)* (11); *(e)* (12); *(f)* (13).

Section S8. Mitochondrial NADPH handling

In this section we will provide a detailed description of the mitochondrial NADPH handling.

$$NADPm = C_{NADPm} - [NADPH]_m \tag{S50}$$

$$V_{IDP\_NADP} = \left(1+\frac{[H^+]_m}{k^{H+}_{m\_IDP}}\right)\left(\begin{array}{l} 1+\frac{[ISOC]}{k^{ISOC}_{m\_IDP}}+\frac{NADP_m}{k^{NADP}_{m\_IDP}}\left(1+\frac{k^{NADP}_{i\_IDP}}{NADP_m}\right)+\frac{[aKG]}{k^{aKG}_{m\_IDP}}+\frac{[NADPH_m]}{k^{NADPH}_{m\_IDP}}+\ldots \\ \ldots\frac{[ISOC]}{k^{ISOC}_{m\_IDP}}\frac{NADP_m}{k^{NADP}_{m\_IDP}}\left(1+\frac{k^{NADP}_{i\_IDP}}{NADP_m}\right)+\frac{[aKG]}{k^{aKG}_{m\_IDP}}\frac{[NADPH_m]}{k^{NADPH}_{m\_IDP}}+\ldots \\ \ldots\frac{[ISOC]}{k^{ISOC}_{m\_IDP}}\frac{[NADPH_m]}{k^{NADPH}_{m\_IDP}}+\frac{[aKG]}{k^{aKG}_{m\_IDP}}\frac{NADP_m}{k^{NADP}_{m\_IDP}}\left(1+\frac{k^{NADP}_{i\_IDP}}{NADP_m}\right) \end{array}\right) \tag{S51}$$

$$V_{IDH_{NADP}} = \frac{V^{IDH}_f\frac{k[ISOC]}{k^{ISOC}_{m\_IDP}}\frac{NADP_m}{k^{NADP}_{m\_IDP}}\left(1+\frac{k^{NADP}_{i\_IDP}}{VNADH_m}\right)-V^{IDH}_b\frac{[aKG]}{k^{aKG}_{m\_IDP}}\frac{[NADP_m]}{k^{NADPH}_{m\_IDP}}}{V_{IDP\_NADP}} \tag{S52}$$

$$V_{THDen} = 1 + \frac{[NADH_m]}{k_{m\_THD}^{NADHm}} + \frac{NAD}{k_{m\_THD}^{NAD}} + \frac{NADP_m}{k_{m\_THD}^{NADP}} + \frac{[NADPH_m]}{k_{m\_THD}^{NADPH}} + \frac{[NADH_m]}{k_{m\_THD}^{NADHm}} \frac{NADP_m}{k_{m\_THD}^{NADP}} e^{(F/10RT).\Delta\mu_H} + \frac{[NADPH_m]}{k_{m\_THD}^{NADPH}} \frac{[NADH_m]}{k_{m\_THD}^{NADHm}} e^{(1-(F/10RT).\Delta\mu_H)} + \frac{NAD}{k_{m\_THD}^{NAD}} \frac{NADP_m}{k_{m\_THD}^{NADP}} e^{(F/10RT).\Delta\mu_H} . e^{(1-(F/10RT).\Delta\mu_H)} + \frac{[NADH_m]}{k_{m\_THD}^{NADHm}} \frac{[NADPH_m]}{k_{m\_THD}^{NADPH}} \quad \text{(S53)}$$

$$V_{THD} = \frac{E_T^{THD}.k_a^{THD} \frac{[NADH]_m}{k_{m\_THD}^{NADHm}} \frac{NADP_m}{k_{m\_THD}^{NADP}} e^{(F/10RT).\Delta\mu_H} - E_T^{THD}.k_b^{THD} \frac{NAD}{k_{m\_THD}^{NAD}} \frac{[NADPH_m]}{k_{m\_THD}^{NADPH}} e^{(1-(F/10RT).\Delta\mu_H)}}{V_{THDen}} \quad \text{(S54)}$$

Table S3. Parameter values used in the simulations: Mitochondrial NADPH handling

Symbol	Value	Units	Description	Eq.	Reference
C_{NADPm}	0.1	mM	Sum of NADPH plus $NADP^+$	S50	
$k_{m\_IDP}^{H+}$	0.5	mM	Dissociation constant for H^+ of IDH2	S51	
$k_{m\_IDP}^{ISOC}$	3.9×10^{-3}	mM	Michaelis constant for ISOC in IDH2	S51,S52	
$k_{m\_IDP}^{NADP}$	6.7×10^{-3}	mM	Michaelis constant for NADP in IDH2	S51,S52	
$k_{i\_IDP}^{NADP}$	2×10^{-6}	mM	Inhibition constant for NADP in IDH2	S51,S52	
$k_{m\_IDP}^{NADPH}$	1.2×10^{-2}	mM	Michaelis constant for NADPH in IDH2	S51,S52	
$k_{m\_IDP}^{aKG}$	0.51	mM	Michaelis constant for αKG in IDH2	S51,S52	
V_f^{IDH}	8.7×10-5	mM ms^{-1}	Maximal rate of IDH2 in the forward direction	S52	
V_{fb}^{IDH}	5.45×10^{-6}	mM ms^{-1}	Maximal rate of IDH2 in the reverse direction	S52	
$k_{m\_THD}^{NADPH}$	0.02	mM	Michaelis constant for NADPH in transhydrogenase (THD)	S53,S54	
$k_{m\_THD}^{NADHm}$	0.01	mM	Michaelis constantfor NADH in THD	S53,S54	
$k_{m\_THD}^{NAD}$	0.125	mM	Michaelis constant for NAD in THD	S53,S54	

$k_{m\_THD}^{NADP}$	0.017	mM	Michaelis constant for NADP in THD	S53,S54
E_T^{THD}	1.187×10^{-5}	mM	Concentration of THD enzyme	S54
k_a^{THD}	1.17474	ms^{-1}	Forward catalytic constant of THD	S54
k_b^{THD}	10	ms^{-1}	Reverse catalytic constant of THD	S54

Section S9. Mitochondrial Model of Energy Metabolism and ion dynamics

The detailed explanation of the mathematical expressions and parameters of the model were previously presented in Wei et al. (2011).

9.1. Computational modeling of Na^+/H^+ exchanger (NHE) and phosphate carrier (PiC)

$$J_{NHE} = c_{NHE}\frac{\beta_1^+\beta_2^+ - \beta_1^-\beta_2^-}{\beta_1^+ + \beta_1^- + \beta_2^+ + \beta_2^-}\frac{}{1+10^{n_i(pH_i - pK_i)}}$$

where

$$\beta_1^+ = \frac{k_1^+ K_{H\_NHE}[Na^+]_m}{K_{H\_NHE}[Na^+]_m + K_{H\_NHE}K_{Na\_NHE} + K_{Na\_NHE}[H^+]_m}$$

$$\beta_2^+ = \frac{k_4^+ K_{Na\_NHE}[H^+]_i}{K_{H\_NHE}[Na^+]_i + K_{H\_NHE}K_{Na\_NHE} + K_{Na\_NHE}[H^+]_i}$$

$$\beta_1^- = \frac{k_1^- K_{H\_NHE}[Na^+]_i}{K_{H\_NHE}[Na^+]_i + K_{H\_NHE}K_{Na\_NHE} + K_{Na\_NHE}[H^+]_i}$$

$$\beta_2^- = \frac{k_4^- K_{Na\_NHE}[H^+]_m}{K_{H\_NHE}[Na^+]_m + K_{H\_NHE}K_{Na\_NHE} + K_{Na\_NHE}[H^+]_m}$$

$$J_{PIC} = c_{PiC}\frac{V_{PIC,f}\frac{[H_2PO_4^{2-}]_i[OH^-]_m}{K_{Pi,i}K_{OH,m}} - V_{PIC,b}\frac{[H_2PO_4^{2-}]_m[OH^-]_i}{K_{Pi,m}K_{OH,i}}}{\left(1+\frac{[H_2PO_4^{2-}]_i}{K_{Pi,i}}+\frac{[OH^-]_m}{K_{OH,m}}+\frac{[H_2PO_4^{2-}]_m}{K_{Pi,m}}+\frac{[OH^-]_i}{K_{OH,i}}+\frac{[H_2PO_4^{2-}]_m[OH^-]_i}{K_{Pi,m}K_{OH,i}}+\frac{[H_2PO_4^{2-}]_i[OH^-]_m}{K_{Pi,i}K_{OH,m}}\right)}$$

Table S4. **Parameter values for the mitochondrial Na^+/H^+ proton exchanger and phosphate carrier**

Symbol	Value	Units	Description
k_1^+	0.0252	ms^{-1}	NHE forward rate constant
k_1^-	0.0429	ms^{-1}	NHE backward rate constant
k_4^+	0.16	ms^{-1}	NHE forward rate constant
k_4^-	0.0939	ms^{-1}	NHE backward rate constant
K_{Na_NHE}	24	mM	Na+Dissociation constant
K_{H_NHE}	1.585×10^{-4}	mM	H+Dissociation constant
pK_i	8.52		Proton inhibitory constant
n_i_NHE	3		Hill coefficient for H+ binding
c_{NHE}	0.00785 (mitochondria)	mM	NHE concentration
$K_{Pi,i}$	11.06	mM	Extra-matrix Pi binding constant
$K_{Pi,m}$	11.06	mM	Mitochondrial matrix Pi binding constant
$K_{OH,i}$	4.08×10^{-5}	mM	Extra-matrix OH- binding constant
$K_{OH,m}$	4.08×10^{-5}	mM	Mitochondrial matrix OH- binding constant
$V_{PIC,f}$	90	μmol min^{-1} mg $protein^{-1}$	Forward V_{max} of phosphate carrier
$V_{PIC,b}$	90	μmol min^{-1} mg $protein^{-1}$	Backward V_{max} of phosphate carrier
c_{PiC}	1.6915 (mitochondria)	mg protein ml^{-1}	PiC concentration

9.2. TCA cycle rate equations

$$V_{CS} = \frac{k_{cat}^{CS} E_T^{CS}}{\left(1+\frac{K_M^{AcCoA}}{[AcCoA]}\right)\left(1+\frac{K_M^{OAA}}{[OAA]}\right)}$$

$$V_{ACO} = k_f^{ACO}\left([CIT] - \frac{[ISOC]}{K_E^{ACO}}\right)$$

$$V_{IDH} = k_{cat}^{IDH} E_T^{IDH}\left[\begin{array}{l}\left(1+\frac{[H^+]_m}{k_{h,1}}+\frac{k_{h,2}}{[H^+]_m}\right)+ f_i^{IDH}\left(\frac{K_{Midh}^{NAD}}{[NAD]}\right)+\ldots \\ f_a^{IDH}\left(\frac{K_M^{ISOC}}{[ISOC]}\right)^{ni} + f_a^{IDH} f_i^{IDH}\left(\frac{K_M^{ISOC}}{[ISOC]}\right)^{ni}\left(\frac{K_{Midh}^{NAD}}{[NAD]}\right)\end{array}\right]^{-1}$$

$$f_a^{IDH} = \left[\left(1+\frac{[ADP^{3-}]_m}{K_{ADP}^a}\right)\left(1+\frac{[Ca^{2+}]_m}{K_{Ca}^a}\right)\right]^{-1}$$

$$f_i^{IDH} = \left(1+\frac{[NADH]}{K_{i,NADH}}\right)$$

$$V_{KGDH} = \frac{k_{cat}^{KGDH} E_T^{KGDH}}{1+\frac{[H^+]_m}{k_{h,1a}}+\frac{k_{h,2a}}{[H^+]_m}+ f_a^{KGDH}\left(\frac{k_M^{\alpha KG}}{[\alpha KG]}\right)^{n_{\alpha KG}} + f_a^{KGDH}\frac{k_{M\_kgdh}^{NAD}}{[NAD]}}$$

$$f_a^{KGDH} = \left[\left(1+\frac{[Mg^{2+}]}{K_D^{Mg^{2+}}}\right)\left(1+\frac{[Ca^{2+}]_m}{K_D^{Ca^{2+}}}\right)\right]^{-1}$$

$$V_{SL} = k_f^{SL}\left([SCoA][ADP]_m[Pi]_m - \frac{[Suc][ATP]_m[CoA]}{K_{E,app}^{SL}}\right)$$

$$K_{E,app}^{SL} = K_{Eq}^{SL}\frac{P_{SUC}P_{ATP}}{P_{Pi}P_{ADP}}$$

Succinate dehydrogenase is included in the Table comprising the respiratory complexes

$$V_{FH} = k_f^{FH}\left([FUM] - \frac{[MAL]}{K_E^{FH}}\right)$$

$$V_{MDH} = \frac{k_{cat}^{MDH} E_T^{MDH} f_{h,a} f_{h,i}}{1 + \frac{K_M^{MAL}}{[MAL]}\left(1 + \frac{[OAA]}{K_i^{OAA}}\right) + \frac{K_M^{NAD}}{[NAD]} + \frac{K_M^{MAL}}{[MAL]}\left(1 + \frac{[OAA]}{K_i^{OAA}}\right)\frac{K_M^{NAD}}{[NAD]}}$$

$$f_{h,a} = \left(1 + \frac{[H^+]}{k_{h1}} + \frac{[H^+]^2}{k_{h1}k_{h2}}\right)^{-1} + k_{offset}$$

$$f_{h,i} = \left(1 + \frac{k_{h3}}{[H^+]} + \frac{k_{h3}k_{h4}}{[H^+]^2}\right)$$

$$V_{AAT} = k_f^{AAT}[OAA][GLU]\frac{k_{ASP}K_E^{ATT}}{\left(k_{ASP}K_E^{AAT} + [\alpha KG]k_f^{AAT}\right)}$$

Table S5. Parameter values used in the simulations: Tricarboxylic acid cycle

Symbol	Value	Units	Description
[AcCoA]	1×10^{-6}-1	mM	Acetyl CoA concentration
k_{cat}^{CS}	7.841×10^{-6}	ms^{-1}	Catalytic constant of CS
E_T^{CS}	0.4	mM	Concentration of CS
K_M^{AcCoA}	0.0126	mM	Michaelis constant for AcCoA
K_M^{OAA}	6.4×10^{-4}	mM	Michaelis constant for OAA
$C_{k\,\mathrm{int}}$	1.3	mM	Sum of TCA cycle intermediates
k_f^{ACO}	3.896×10^{-6}	ms^{-1}	Forward rate constant of ACO
K_E^{ACO}	2.22		Equilibrium constant of ACO
$K_{i,NADH}$	0.19	mM	Inhibition constant by NADH
k_{cat}^{IDH}	0.0264	ms^{-1}	Rate constant of IDH

E_T^{IDH}	0.109	mM	Concentration of IDH
$k_{h,1}$	1×10^{-5}	mM	Inoization constant of IDH
$k_{h,2}$	9×10^{-4}	mM	Inoization constant of IDH
K_M^{ISOC}	1.52	mM	Michaelis constant for isocitrate
n_i	2.0		Cooperativity for isocitrate
K_{Midh}^{NAD}	0.923	mM	Michaelis constant for NAD^+
K_{ADP}^a	0.62	mM	Activation constant by ADP
K_{Ca}^a	5×10^{-4}	mM	IDH activation constant for Ca^{2+}
E_T^{KGDH}	0.5	mM	Concentration of KGDH
k_{cat}^{KDGH}	8.83×10^{-4}	ms^{-1}	Rate constant of KGDH
$k_M^{\alpha KG}$	30	mM	Michaelis constant for αKG
$K_{M\_kgdh}^{NAD}$	38.7	mM	Michaelis constant for NAD^+ of KGDH
$k_{h,1a}$	4×10^{-5}	mM	Ionization constant of KGDH
$k_{h,2a}$	7×10^{-5}	mM	Ionization constant of KGDH
$K_D^{Mg^{2+}}$	0.0308	mM	Activation constant for Mg^{2+}
$K_D^{Ca^{2+}}$	1.5×10^{-4}	mM	Activation constant for Ca^{2+}
$n_{\alpha KG}$	1.2		Hill coefficient of KGDH for α KG
$[Mg^{2+}]_m$	0.4	mM	Mg^{2+} concentration in mitochondria
$[Mg^{2+}]_i$	1.0	mM	Mg^{2+} concentration in cytosol/buffer
k_f^{SL}	1.4×10^{-3}	$mM^{-1}ms^{-1}$	Forward rate constant of SL
K_E^{SL}	3.115		Equilibrium constant of the SL reaction

[CoA]	0.02	mM	Coenzyme A concentrations.
k_f^{FH}	4.15×10^{-4}	ms^{-1}	Forward rate constant for FH.
K_E^{FH}	1.0		Equilibrium constant of FH
k_{h1}	1.131×10^{-5}	mM	Ionization constant of MDH
k_{h2}	26.7	mM	Ionization constant of MDH
k_{h3}	6.68×10^{-9}	mM	Ionization constant of MDH
k_{h4}	5.62×10^{-6}	mM	Ionization constant of MDH
k_{offset}	3.99×10^{-2}		Offset of MDH pH activation factor
k_{cat}^{MDH}	6.21×10^{-3}	ms^{-1}	Rate constant of MDH
E_T^{MDH}	0.154	mM	Total MDH enzyme concentration
K_M^{MAL}	1.493	mM	Michaelis constant for malate
K_i^{OAA}	0.031	mM	Inhibition constant for oxalacetate
K_M^{NAD}	0.2244	mM	Michaelis constant for NAD^+
[GLU]	$1\times10^{-4} \sim 30$	mM	Glutamate concentration.
k_f^{AAT}	1.07×10^{-3}	ms^{-1}	Forward rate constant of AAT
K_E^{AAT}	6.6		Equilibrium constant of AAT
k_{ASP}	1.5×10^{-6}	ms^{-1}	Rate constant of aspartate consumption

9.3. Oxidative Phosphorylation rate equations

$$V_{O_2} = 0.5\rho^{res}\frac{\left(r_a + r_{c1}e^{\left(\frac{6F\Delta\Psi_B}{RT}\right)}\right)e^{\left(\frac{FA_{res}}{RT}\right)} - r_a e^{\left(\frac{g6F\Delta\mu_H}{RT}\right)} + r_{c2}e^{\left(\frac{FA_{res}}{RT}\right)}e^{\left(\frac{g6F\Delta\mu_H}{RT}\right)}}{\left(1 + r_1 e^{\left(\frac{FA_{res}}{RT}\right)}\right)e^{\left(\frac{6F\Delta\Psi_B}{RT}\right)} + \left(r_2 + r_3 e^{\left(\frac{FA_{res}}{RT}\right)}\right)e^{\left(\frac{g6F\Delta\mu_H}{RT}\right)}}$$

$$V_{He} = 6\rho^{res} \frac{\left(r_a e^{\left(\frac{A_{res}F}{RT}\right)} - (r_a + r_b) e^{\left(\frac{g6F\Delta\mu_H}{RT}\right)} \right)}{\left(1 + r_1 e^{\left(\frac{FA_{res}}{RT}\right)}\right) e^{\left(\frac{6F\Delta\Psi_B}{RT}\right)} + \left(r_2 + r_3 e^{\left(\frac{FA_{res}}{RT}\right)}\right) e^{\left(\frac{g6F\Delta\mu_H}{RT}\right)}}$$

$$A_{res} = \frac{RT}{F} \ln\left(K_{res} \sqrt{\frac{[NADH]}{[NAD^+]}} \right)$$

$$V_{O_2SDH} = 0.5\rho^{res(SDH)} \frac{\left(r_a + r_{c1} e^{\left(\frac{4F\Delta\Psi_B}{RT}\right)}\right) e^{\left(\frac{FA_{RSDH}}{RT}\right)} - r_a e^{\left(\frac{g4F\Delta\mu_H}{RT}\right)} + r_{c2} e^{\left(\frac{FA_{RSDH}}{RT}\right)} e^{\left(\frac{g4F\Delta\mu_H}{RT}\right)}}{\left(1 + r_1 e^{\left(\frac{FA_{RSDH}}{RT}\right)}\right) e^{\left(\frac{4F\Delta\Psi_B}{RT}\right)} + \left(r_2 + r_3 e^{\left(\frac{FA_{RSDH}}{RT}\right)}\right) e^{\left(\frac{g4F\Delta\mu_H}{RT}\right)}} \left(\frac{1}{1 + \frac{[OAA]}{K_i^{OAA}}} \right)$$

$$V_{He(SDH)} = 4\rho^{res(SDH)} \frac{\left(r_a e^{\left(\frac{A_{RSDH}F}{RT}\right)} - (r_a + r_b) e^{\left(\frac{g4F\Delta\mu_H}{RT}\right)} \right)}{\left(1 + r_1 e^{\left(\frac{FA_{RSDH}}{RT}\right)}\right) e^{\left(\frac{4F\Delta\Psi_B}{RT}\right)} + \left(r_2 + r_3 e^{\left(\frac{FA_{RSDH}}{RT}\right)}\right) e^{\left(\frac{g4F\Delta\mu_H}{RT}\right)}} \left(\frac{1}{1 + \frac{[OAA]}{K_i^{OAA}}} \right)$$

$$A_{RSDH} = \frac{RT}{F} \ln\left(K_{RSDH,app} \sqrt{\frac{[SUC]}{[FUM]}} \right)$$

$$K_{RSDH,app} = \frac{K_{res(SDH)}}{P_{SUC}}$$

$$V_{ATPase} = -\rho^{F1} \frac{\left(100 p_a + p_{c1} \exp(3F\Delta\Psi_B / RT)\right) \exp(A_{F1}F / RT) - \left(\begin{array}{l} p_a \exp(3F\Delta\mu_H / RT) \\ \cdots + p_{c2} \exp(A_{F1}F / RT) \exp(3F\Delta\mu_H / RT) \end{array} \right)}{\left(1 + p_1 \exp(A_{F1}F / RT)\right) \exp(3F\Delta\Psi_B / RT) + \left(p_2 + p_3 \exp(A_{F1}F / RT)\right) \exp(3F\Delta\mu_H / RT)}$$

$$V_{Hu} = -3\rho^{F1} \frac{p_a \left(1 + \exp(A_{F1}F / RT)\right) - \left(p_a + p_b\right) \exp(3F\Delta\mu_H / RT)}{\left(1 + p_1 \exp(A_{F1}F / RT)\right) \exp(3F\Delta\Psi_B / RT) + \left(p_2 + p_3 \exp(A_{F1}F / RT)\right) \exp(3F\Delta\mu_H / RT)}$$

$$A_{F1} = \frac{RT}{F} \ln\left(K_{app}^{ATPase} \frac{[MgATP^{2-}]}{[ADP_{free}][Pi_{total}]}\right)$$

$$K_{app}^{ATPase} = K_{eq}^{ATPase}[H^+]^1 \frac{P_{ATP}P_{H_2O}}{P_{ADP}P_{Pi}}$$

Table S6. Parameter values used in the simulations: Oxidative phosphorylation

Symbol	Value	Units	Description
r_a	6.394×10^{-13}	ms^{-1}	Sum of products of rate constants
r_b	1.762×10^{-16}	ms^{-1}	Sum of products of rate constants
r_{c1}	2.656×10^{-22}	ms^{-1}	Sum of products of rate constants
r_{c2}	8.632×10^{-30}	ms^{-1}	Sum of products of rate constants
r_1	2.077×10^{-18}		Sum of products of rate constants
r_2	1.728×10^{-9}		Sum of products of rate constants
r_3	1.059×10^{-26}		Sum of products of rate constants
ρ^{res}	T.1	mM	Concentration of electron carriers (respiratory complexes I-III-IV)
K_{res}	1.35×10^{18}		Equilibrium constant of respiration
$\rho^{res(SDH)}$	T.1	mM	Concentration of electron carriers (respiratory complexes II-III-IV)
$\Delta\Psi_B$	50	mV	Phase boundary potential
g	0.85		Correction factor for voltage
K_I^{OAA}	0.15		Inhibition constant for OAA
$K_{res(SDH)}$	5.765×10^{13}		Equilibrium constant of SDH
p_a	1.656×10^{-8}	ms^{-1}	Sum of products of rate constants
p_b	3.373×10^{-10}	ms^{-1}	Sum of products of rate constants
p_{c1}	9.651×10^{-17}	ms^{-1}	Sum of products of rate constants
p_{c2}	4.585×10^{-17}	ms^{-1}	Sum of products of rate constants

p_1	1.346×10^{-4}		Sum of products of rate constants
p_2	7.739×10^{-7}		Sum of products of rate constants
p_3	6.65×10^{-15}		Sum of products of rate constants
ρ^{F1}	T.1	mM	Concentration of F_1F_0-ATPase
K_{eq}^{ATPase}	1.71×10^{6}		Equilibrium constant of ATP synthesis
$[Pi]_i$	T.1	mM	Inorganic phosphate concentration
C_A	1.5	mM	Total sum of adenine nucleotides
V_{maxANT}	T.1	mM ms^{-1}	Maximal rate of the ANT
h^{ANT}	0.5		Fraction of $\Delta\Psi_B$
g_H	T.1	mM ms^{-1} mV^{-1}	Ionic conductance of the inner membrane
C_{PN}	1.0	mM	Total sum of pyridine nucleotides
C_{mito}	1.812×10^{-3}	mM mV^{-1}	Inner membrane capacitance

9.4. Acid-base equilibria of adenine nucleotides and phosphate

Chemical species in the biochemical reactions exist in mixed ionic forms such as protonated, deprotonated or bound to different cations (14-17). In general, the total concentration of ligand is the sum of free ligand, ligand bound to proton and to metals (17).

$$[L_{total}] = [L] + \sum_{P=1}^{N_P} [LH_P] + \sum_{m=1}^{N_m} [LM^m]$$

where L is the ligand, H is the proton and M^m is the m^{th} metal ion. The second term on the right hand side of the eqn. refers to the sum of the protonated moieties, and the third term represents the sum of the metal-bound moieties. Therefore, N_P is the total number of protonation sites, and N_m is the total number of metal-binding sites in the ligand.

Here, only the most abundant and physiological significant forms of ATP, ADP, and phosphate in the pH range from 5.0 to 9.0 were considered: ATP^{4-}, $HATP^{3-}$, $MgATP^{-}$, ADP^{3-}, $HADP^{2-}$, $MgADP^{-}$, HPO_4^{2-}, and $H_2PO_4^{-}$.

$$[ATP^{4-}]_m = \frac{[ATP_{total}]_m}{\left(1 + \frac{[H^+]_m}{K_{a,ATP}} + \frac{[Mg^{2+}]_m}{K_{Mg,ATP}}\right)}$$

$$[HATP^{3-}]_m = \frac{[ATP^{4-}]_m[H^+]_m}{K_{a,ATP}}$$

$$[MgATP^{2-}]_m = \frac{[ATP^{4-}]_m[Mg^{2+}]_m}{K_{Mg,ATP}}$$

$$[ADP^{3-}]_m = \frac{[ADP_{total}]_m}{\left(1 + \frac{[H^+]_m}{K_{a,ADP}} + \frac{[Mg^{2+}]_m}{K_{Mg,ADP}}\right)}$$

$$[HADP^{2-}]_m = \frac{[ADP^{3-}]_m[H^+]_m}{K_{a,ADP}}$$

$$[MgADP^{-}]_m = \frac{[ADP^{3-}]_m[Mg^{2+}]_m}{K_{Mg,ADP}}$$

$$[H_2PO_4^-]_m = \frac{[Pi]_{total}}{1 + \frac{[H^+]_m}{K_{a,Pi}}}$$

$$[HPO_4^{2-}]_m = \frac{[H_2PO_4^-]_m K_{a,Pi}}{[H^+]_m}$$

$$[ATP^{4-}]_i = \frac{[ATP_{total}]_i}{\left(1 + \frac{[H^+]_i}{K_{a,ATP}} + \frac{[Mg^{2+}]_i}{K_{Mg,ATP}}\right)}$$

$$[ADP^{3-}]_i = \frac{[ADP_{total}]_i}{\left(1 + \frac{[H^+]_i}{K_{a,ADP}} + \frac{[Mg^{2+}]_i}{K_{Mg,ADP}}\right)}$$

$$[ATP_{total}] = [ATP^{4-}] + [HATP^{3-}] + [MgATP^{-}]$$

$$[ATP_{free}] = [ATP^{4-}] + [HATP^{3-}]$$

$$[ADP_{free}] = [ADP^{3-}] + [HADP^{2-}]$$

$$[Pi_{total}] = [H_2Pi^{-}] + [H\ Pi^{2-}]$$

9.5. Polynomials for species undergoing acid-base equilibrium, ionic gradients, and conservation relations

$$P_{ATP} = 1 + \frac{[H^+]_m}{K_{a,ATP}} + \frac{[Mg^{2+}]_m}{K_{Mg,ATP}}$$

$$P_{ADP} = 1 + \frac{[H^+]_m}{K_{a,ADP}} + \frac{[Mg^{2+}]_m}{K_{Mg,ADP}}$$

$$P_{Pi} = 1 + \frac{[H^+]_m}{K_{a,Pi}}$$

$$P_{SUC} = 1 + \frac{[H^+]_m}{K_{a,SUC}}$$

$$P_{H_2O} = 1 + \frac{[H^+]_m}{K_{a,H_2O}}$$

$$\Delta\mu_H = -2.303\frac{RT}{F}\Delta pH + \Delta\Psi_m$$

$$\Delta pH = pH_i - pH_m$$

$$\Delta\Psi_m = \Psi_i - \Psi_m$$

$$[NAD^+] = C_{PN} - [NADH]$$

$$[ATP_{total}] = C_A - [ADP_{total}]$$

9.6. Adenine Nucleotide translocator (ANT)

$$V_{ANT} = \mathrm{V}_{\mathrm{maxANT}} \frac{\left(1 - \frac{[ATP^{4-}]_i \times [ADP^{3-}]_m}{[ADP^{3-}]_i \times [ATP^{4-}]_m}\right)\exp(-F\Delta\Psi_m / RT)}{\left(1 + \frac{[ATP^{4-}]_i}{[ADP^{3-}]_i}\exp(-hF\Delta\Psi / RT)\right)\left(1 + \frac{[ADP^{3-}]_m}{[ATP^{4-}]_m}\right)}$$

9.7. Ionic fluxes rate equations

$$V_{uni} = V_{\max}^{uni} \frac{\frac{[Ca^{2+}]_i}{K_{trans}}\left(1+\frac{[Ca^{2+}]_i}{K_{trans}}\right)^3 \frac{2F\left(\Delta\Psi_m - \Delta\Psi^\circ\right)}{RT}}{\left(\left(1+\frac{[Ca^{2+}]_i}{K_{trans}}\right)^4 + \frac{L}{\left(1+\frac{[Ca^{2+}]_i}{K_{act}}\right)^{n_a}}\right)\left(1-e^{\left(\frac{-2F\left(\Delta\Psi_m-\Delta\Psi^\circ\right)}{RT}\right)}\right)}$$

$$V_{NaCa} = V_{\max}^{NaCa} \frac{e^{\left(\frac{bF\left(\Delta\Psi_m-\Delta\Psi^\circ\right)}{RT}\right)} e^{\left(\ln\frac{[Ca^{2+}]_m}{[Ca^{2+}]_i}\right)}}{\left(1+\frac{K_{Na}}{[Na^+]_i}\right)^n \left(1+\frac{K_{Ca}}{[Ca^{2+}]_m}\right)}$$

$$J_{NHE} = c_{NHE} \frac{\frac{\beta_1^+\beta_2^+ - \beta_1^-\beta_2^-}{\beta_1^+ + \beta_1^- + \beta_2^+ + \beta_2^-}}{1+10^{n_i(pH_i - pK_i)}}$$

$$\beta_1^+ = \frac{k_1^+ K_{H\_NHE}[Na^+]_m}{K_{H\_NHE}[Na^+]_m + K_{H\_NHE}K_{Na\_NHE} + K_{Na\_NHE}[H^+]_m}$$

$$\beta_2^+ = \frac{k_2^+ K_{Na\_NHE}[H^+]_i}{K_{H\_NHE}[Na^+]_i + K_{H\_NHE}K_{Na\_NHE} + K_{Na\_NHE}[H^+]_i}$$

$$\beta_1^- = \frac{k_1^- K_{H\_NHE}[Na^+]_i}{K_{H\_NHE}[Na^+]_i + K_{H\_NHE}K_{Na\_NHE} + K_{Na\_NHE}[H^+]_i}$$

$$\beta_2^- = \frac{k_2^- K_{Na\_NHE}[H^+]_m}{K_{H\_NHE}[Na^+]_m + K_{H\_NHE}K_{Na\_NHE} + K_{Na\_NHE}[H^+]_m}$$

$$J_{PIC} = c_{PiC} \frac{V_{PIC,f}\frac{[HPO_4^{2-}]_i[OH^-]_m}{K_{Pi,i}K_{OH,m}} - V_{PIC,b}\frac{[HPO_4^{2-}]_m[OH^-]_i}{K_{Pi,m}K_{OH,i}}}{\left(1+\frac{[HPO_4^{2-}{}_i}{K_{Pi,i}} + \frac{[OH^-]_m}{K_{OH,m}} + \frac{[HPO_4^{2-}]_m}{K_{Pi,m}} + \frac{[OH^-]_i}{K_{OH,i}} + \frac{[HPO_4^{2-}]_m[OH^-]_i}{K_{Pi,m}K_{OH,i}} + \frac{[HPO_4^{2-}]_i[OH^-]}{K_{Pi,i}K_{OH,m}}\right.}$$

$$V_{Hleak} = g_H \Delta\mu_H$$

9.8. pH regulation in the mitochondria

Apparent equilibrium constant is defined in terms of the species concentration at equilibrium and as a function of pH (17).

$$K' = [H^+]^n \frac{K_{ref} \prod P_{product}}{\prod P_{reactant}}$$

where n is proton stoichiometry of the reference reaction and P is the binding polynomial ($P=1+\sum_{P=1}^{N_P} \frac{[H]^P}{\prod_{l=1}^{P} K_{a,l}} + \sum_{m=1}^{N_m} \frac{[M^m]}{K_{M^m}}$). K_{ref} is the equilibrium constant for the reference reaction ($K_{ref} = e^{-\Delta_r G^0/RT}$).

9.9. pH-dependence of TCA cycle enzyme activities

$$V_{KGDH} = \frac{k_{cat}^{KGDH} k_T^{KGDH}}{1 + \frac{[H^+]_m}{k_{h,1a}} + \frac{k_{h,2a}}{[H^+]_m} + f_a^{KGDH} \left(\frac{k_M^{\alpha KG}}{[\alpha KG]} \right)^{n_{\alpha KG}} + f_a^{KGDH} \frac{k_M^{NAD}}{[NAD]}}$$

$$f_a^{KGDH} = \left[\left(1 + \frac{[Mg^{2+}]}{K_D^{Mg^{2+}}} \right) \left(1 + \frac{[Ca^{2+}]_m}{K_D^{Ca^{2+}}} \right) \right]^{-1}$$

9.10. Parameter values used in the simulations of ion handling

Table S7. Parameter values used in the simulations: Mitochondrial Ca^{2+} handling

Symbol	Value	Units	Description
V_{max}^{uni}	T.1	mM ms^{-1}	V_{max}uniporter Ca^{2+} transport
$\Delta\Psi^\circ$	91	mV	Offset membrane potential
K_{act}	3.8×10^{-4}	mM	Activation constant
K_{trans}	0.019	mM	K_d for translocated Ca^{2+}

L	110.0		K_{eq} for conformational transitions in uniporter
n_a	2.8		Uniporter activation cooperativity
$V_{\max}^{NaCa}$	T.1	mM ms^{-1}	V_{max} of Na^+/Ca^{2+} exchanger
b	0.5		$\Delta\Psi_m$ dependence on Na^+/Ca^{2+} exchanger
K_{Na}	9.4	mM	Exchanger Na^{2+} constant
K_{Ca}	3.75×10^{-4}	mM	Exchanger Ca^{2+} constant
n	3.0		Na^+/Ca^{2+} exchanger cooperativity
δ_{Ca}	3×10^{-4}		Fraction of free $[Ca^{2+}]_m$

Table S8. Parameter values used in the simulations: Mitochondrial H^+ and Na^+ handling

Symbol	Value	Units	Description
δ_H	$1\times10^{-5*}$	dimensionless	mitochondria H^+ buffering capacity
$K_{a,ADP}$	4.17×10^{-7}		ADP dissociation constant
$K_{a,ATP}$	3.31×10^{-7}		ATP dissociation constant
$K_{a,Pi}$	1.78×10^{-7}		Pi dissociation constant
$K_{Mg,ATP}$	6.46×10^{-5}		Mg^{2+}ATP dissociation constant
$K_{Mg,ADP}$	5.62×10^{-4}		Mg^{2+}ADP dissociation constant
$K_{a,SUC}$	6.3×10^{-6}		Ka of succinate dissociation constant
K_{a,H_2O}	1×10^{-14}	M	dissociation constant for water
$[H^+]_i$	1×10^{-4}	mM	cytosolic H^+ concentration
$[Na^+]_i$	T.1	mM	cytosolic Na^+ concentration
$[Ca^{2+}]_i$	1×10^{-4}	mM	cytosolic Ca^{2+} concentration
$[ADP]_i$	0.01~1.0	mM	cytosolic ADP concentration

*from Nyguyen (18) and Vaughan-Jones (19)

Section S10. ROS transport

$$V_{IMAC} = \left(a + \frac{b}{1 + \frac{K_{cc}}{[O_2^{\bullet -}]_i}} \right) \left(GL + \frac{G_{max}}{1 + e^{\left(K\left(\Delta\Psi_m^b \right) + \Delta\Psi_m \right)}} \right) \Delta\Psi_m$$

$$V_{ROS}^{Tr} = j \frac{V_{IMAC}}{\Delta\Psi_m} \left(-\Delta\Psi_m - \frac{RT}{F} \log\left(\frac{[O_2^{\bullet -}]_m}{[O_2^{\bullet -}]_i} \right) \right)$$

Table S9. Parameter values used in the simulations: ROS transport

Symbol	Value	Units	Description
a	1×10^{-3}	dimensionless	Basal IMAC conductance
b	1×10^{4}	dimensionless	Activation factor by cytoplasmic $O_2^{\cdot -}$
K_{cc}	1×10^{-2}	mM	Activation constant by cytoplasmic $O_2^{\cdot -}$
GL	3.5×10^{-8}		Integral conductance for IMAC
G_{max}	3.9085×10^{-6}		Leak conductance of IMAC at saturation
K	7.0×10^{-2}	mV^{-1}	Steepness factor
$\Delta\Psi_m^b$	4	mV	Potential at half saturation
j	0.1	dimensionless	Fraction of IMAC conductance
$\frac{RT}{F}$	26.730818		

Section **11. State variables initial conditions**

Symbol	Value	Units	Description
$[Ca^{2+}]_m$	2.738×10^{-5}	mM	Mitochondrial matrix Ca^{2+}
$[ADP]_m$	0.0158	mM	Mitochondrial matrix ADP
$\Delta\Psi_m$	193.0	mV	Mitochondrial membrane potential
[NADH]	0.965	mM	Mitochondrial matrix NADH
$[H^+]_m$	6.97×10^{-5}	mM	Mitochondrial matrix H^+
$[Pi]_m$	8.28	mM	Mitochondrial matrix Pi
[ISOC]	0.121	mM	Isocitrate
[αKG]	0.13	mM	α-ketoglutarate
[SCoA]	0.0161	mM	Succinyl CoA
[Suc]	0.037	mM	Succinate
[FUM]	0.235	mM	Fumarate
[MAL]	0.228	mM	Malate
[OAA]	0.00128	mM	Oxalacetate
$[Na^+]$m	0.0985	mM	Mitochondrialmatrix Na^+
$[O_2^{\bullet-}]_m$	6.39×10^{-6}	mM	Mitochondrial matrix Superoxide
$[O_2^{\bullet-}]_i$	4.83×10^{-8}	mM	Extra-matrix Superoxide
$[H_2O_2]_m$	8.23×10^{-5}	mM	Mitochondrial matrix Hydrogen peroxide
$[H_2O_2]_i$	2.83×10^{-7}	mM	Extra-matrix Hydrogen peroxide
$[GSH]_m$	1.65	mM	Mitochondrial matrix GSH
$[GSH]_i$	1.65	mM	Extra-matrix GSH
$[GSSG]_m$	1.32	mM	Mitochondrial matrix GSSG

$[TrxSH_2]_m$	0.0243	mM	Mitochondrial matrix $TrxSH_2$
$[TrxSH_2]_i$	0.0499	mM	Extra-matrix $TrxSH_2$
$[PSSG]_m$	6.76×10^{-4}	mM	Mitochondrial matrix PSSG
$[PSSG]_i$	2.64×10^{-5}	mM	Extra-matrix PSSG

Section S12. Glossary

Symbol	Definition
J_H	Flux of proton transport
K_{ref}^k	Equilibrium constant of k^{th} reference reaction
K_{app}^k	Apparent equilibrium constant of k^{th} reaction
δ_H	Proton buffer capacity
δ_{Ca}	Calcium buffer capacity
αKG	α-ketoglutarate
ASP	Aspartate
CIT	Citric acid
F_1F_o-ATPase	Mitochondrial F_1F_0ATP synthase
FUM	Fumarate
IDH	Isocitrate dehydrogenase
ISOC	Iscocitrate
KGDH	α-ketoglutarate dehydrogenase
MAL	Malate
OAA	Oxalacetate
SCoA	Succinyl CoA

Suc	Succinate
TCA	Tricarboxylic acid cycle
$O_2^{\bullet -}$	Superoxide
H_2O_2	Hydrogen peroxide
GSH	Reduced glutathione
GSSG	Oxidized glutathione
$Trx(SH)_2$	Reduced thioredoxin
TrxSS	Oxidixed thioredoxin
PSSG	Glutathionylated proteins
IDH2	Isocitrate dehydrogenase
THD	Transhydrogenase
V_{AAT}	Rate of aspartate amino transferase
V_{ACO}	Rate of aconitase
V_{ANT}	Rate of the adenine nucleotide transferase
$V_{ATPsynthase}$	Rate of the F_1F_0ATP synthase
V_{CS}	Rate of the citrate synthase
V_{FH}	Rate of the fumarate hydratase
V_{He}	Rate of proton transport driven by complex I, III, and IV
$V_{He(SDH)}$	Rate of proton transport driven by complex II, III and IV
V_{Hleak}	Rate of proton leak across the inner mitochondrial membrane
V_{Hu}	Rate of proton uptake via F_1F_0ATP synthase
V_{IDH}	Rate of isocitrate dehydrogenase

V_{KGDH}	Rate of α-ketoglutarate dehydrogenase
V_{MDH}	Rate of malate dehydrogenase
V_{NaCa}	Rate of the mitochondrial Na^+/Ca^{2+} exchanger
V_{NHE}	Rate of the mitochondrial Na^+/H^+ exchanger
V_{O_2}	Oxygen consumption rate driven by complex I
V_{O_2SDH}	Oxygen consumption rate driven by complex II
V_{PiC}	Rate of the mitochondrial phosphate carrier
V_{SDH}	Rate of succinate dehydrogenase (complex II)
V_{SL}	Rate of succinate lyase
V_{uni}	Rate of Ca^{2+}uniporter in the mitochondrial inner membrane
V_{IMAC}	IMAC conductance
V_{ROS}^{Tr}	Rate of transport of $O_2^{\cdot -}$ across the inner mithochondrial membrane
V_{MnSOD}	Rate of mitochondrial matrix superoxide dismutase
$V_{CuZnSOD}$	Rate of extra-matrixl superoxide dismutase
V_{GPXm}	Rate of mitochondrial matrix glutathione peroxidase
V_{GPXi}	Rate of extra-matrix glutathione peroxidase
V_{GRm}	Rate of mitochondrial matrix glutathione reductase
V_{GR_i}	Rate of extra-matrix glutathione reductase
V_{GRX_m}	Rate of mitochondrial matrix glutaredoxin
V_{GRX_i}	Rate of extra-matrix glutaredoxin
V_{GST}	Rate of extra-matrix GSSG transport

V_{TxPX_m}	Rate of mitochondrial matrix peroxiredoxin
V_{TxPX_i}	Rate of extra-matrix peroxiredoxin
V_{TxR_m}	Rate of mitochondrial matrix thioredoxin reductase
V_{TxR_i}	Rate of extra-matrix thioredoxin reductase
V_{CAT}	Rate of catalase
G/M	Glutamate and malate
DNP	Dinitrophenol
CN	Cyanide
$\Delta\psi_m$	Electric potential across the mitochondrial inner membrane
Δp	Proton motive force
v_m	Volume of the mitochondrial matrix compartment
v_i	Volume of the extra-matrix compartment

References

1. Schafer, F. Q., and G. R. Buettner. 2001. Redox environment of the cell as viewed through the redox state of the glutathione disulfide/glutathione couple. Free Radic Biol Med 30:1191-1212.
2. Aon, M. A., S. Cortassa, E. Marban, and B. O'Rourke. 2003. Synchronized whole cell oscillations in mitochondrial metabolism triggered by a local release of reactive oxygen species in cardiac myocytes. J Biol Chem 278:44735-44744.
3. Cortassa, S., M. A. Aon, R. L. Winslow, and B. O'Rourke. 2004. A mitochondrial oscillator dependent on reactive oxygen species. Biophys J 87:2060-2073.
4. Manoli, I., S. Alesci, M. R. Blackman, Y. A. Su, O. M. Rennert, and G. P. Chrousos. 2007. Mitochondria as key components of the stress response. Trends Endocrinol Metab 18:190-198.
5. Nelson, D. L. 2008. Lehninger principles of biochemistry. W.H. Freeman, New York :.

6. Stanley, B. A., V. Sivakumaran, S. Shi, I. McDonald, D. Lloyd, W. H. Watson, M. A. Aon, and N. Paolocci. 2011. Thioredoxin reductase-2 is essential for keeping low levels of H(2)O(2) emission from isolated heart mitochondria. J Biol Chem 286:33669-33677.
7. Fernandes, A. P., and A. Holmgren. 2004. Glutaredoxins: glutathione-dependent redox enzymes with functions far beyond a simple thioredoxin backup system. Antioxidants & redox signaling 6:63-74.
8. Holmgren, A. 1989. Thioredoxin and glutaredoxin systems. J Biol Chem 264:13963-13966.
9. Cox, A. G., C. C. Winterbourn, and M. B. Hampton. 2010. Mitochondrial peroxiredoxin involvement in antioxidant defence and redox signalling. Biochem J 425:313-325.
10. Sztajer, H., B. Gamain, K. D. Aumann, C. Slomianny, K. Becker, R. Brigelius-Flohe, and L. Flohe. 2001. The putative glutathione peroxidase gene of Plasmodium falciparum codes for a thioredoxin peroxidase. J Biol Chem 276:7397-7403.
11. Pillay, C. S., J. H. Hofmeyr, B. G. Olivier, J. L. Snoep, and J. M. Rohwer. 2009. Enzymes or redox couples? The kinetics of thioredoxin and glutaredoxin reactions in a systems biology context. Biochem J 417:269-275.
12. Eckenroth, B., K. Harris, A. A. Turanov, V. N. Gladyshev, R. T. Raines, and R. J. Hondal. 2006. Semisynthesis and characterization of mammalian thioredoxin reductase. Biochemistry 45:5158-5170.
13. McAdam, M. E., F. Levelle, R. A. Fox, and E. M. Fielden. 1977. A pulse-radiolysis study of the manganese-containing superoxide dismutase from Bacillus stearothermophilus. Biochem J 165:81-87.
14. Alberty, R. A. 2003. Thermodynamics of biochemical reactions. Wiley-Interscience, Hoboken, N.J.
15. Kushmerick, M. J. 1997. Multiple equilibria of cations with metabolites in muscle bioenergetics. Am J Physiol 272:C1739-1747.
16. Alberty, R. A. 2006. Biochemical Thermodynamics: Applications of Mathematica.
17. Vinnakota, K., M. L. Kemp, and M. J. Kushmerick. 2006. Dynamics of muscle glycogenolysis modeled with pH time course computation and pH-dependent reaction equilibria and enzyme kinetics. Biophysical journal 91:1264-1287.
18. Nguyen, M. H., S. J. Dudycha, and M. S. Jafri. 2007. Effect of Ca2+ on cardiac mitochondrial energy production is modulated by Na+ and H+ dynamics. Am J Physiol Cell Physiol 292:C2004-2020.
19. Vaughan-Jones, R. D., B. E. Peercy, J. P. Keener, and K. W. Spitzer. 2002. Intrinsic H(+) ion mobility in the rabbit ventricular myocyte. J Physiol 541:139-158.